Preliminary description and slope stability analyses of the 2008 Little Salmon Lake and 2007 Mt. Steele landslides, Yukon

Marc-André Brideau[1] and Doug Stead
Earth Science Department, Simon Fraser University, Burnaby, BC

Panya Lipovsky
Yukon Geological Survey, Whitehorse, YT

Michel Jaboyedoff
Université de Lausanne, Lausanne, Switzerland

Christopher Hopkinson
Nova Scotia Community College, Annapolis Valley Campus, NS

Michael Demuth
Geological Survey of Canada, Ottawa, ON

John Barlow
Durham University, Durham, Great Britain

Steve Evans and Keith Delaney
Department of Earth and Environmental Sciences, University of Waterloo, Waterloo, ON

Brideau, M.-A., Stead, D., Lipovsky, P., Jaboyedoff, M., Hopkinson, C., Demuth, M., Barlow, J., Evans, S. and Delaney, K., 2010. Preliminary description and slope stability analyses of the 2008 Little Salmon Lake and 2007 Mt. Steele landslides, Yukon. *In:* Yukon Exploration and Geology 2009, K.E. MacFarlane, L.H. Weston and L.R. Blackburn (eds.), Yukon Geological Survey, p. 119-133.

ABSTRACT

In August 2008, reactivation of the Little Salmon Lake landslide occurred. During this event, hundreds of conical mounds of variable size and composition formed in the deposition zone. The characteristics of these landforms are described and a potential mechanism for their formation is proposed. A preliminary slope stability analysis of the 2007 Mount Steele rock and ice avalanche was also undertaken. The orientation of very high persistence (>20 m long) structural planes (*e.g.*, faults, joints and bedding) within bedrock in the source zone was obtained using an airborne-LiDAR digital elevation model and the software COLTOP-3D. Using these discontinuity orientation measurements, kinematic, surface wedge and simple three-dimensional distinct element slope stability analyses were performed.

[1]*mbrideau@sfu.ca*

THE LITTLE SALMON LAKE LANDSLIDE REACTIVATION

INTRODUCTION

The Little Salmon Lake landslide is located on a moderately steep (15°-25°) north-facing slope on the south shore of Little Salmon Lake (Figs. 1, 2). The landslide has been previously described by Lyle (Lyle *et al.*, 2005; Lyle, 2006) who suggested that it originated as a deep-seated rotational bedrock slump prior to 1949. In recent years, rockfall activity was observed at the headscarp and the disintegrated slump blocks have moved noticeably since 1989 (Lyle, 2006). The headscarp of an older landslide is located 250 m above the currently active headscarp. Lyle (2006) suggested that the Little Salmon Lake landslide occurs within this larger relict landslide, and noted graphitic layers in the bedrock which may have formed part of the original failure plane.

The former landslide debris was reactivated in a large debris flow/avalanche some time between August 22 and 28, 2008 following a period of higher than normal precipitation. The 2008 reactivation involved little additional material from the headscarp. Instead, bedrock slump blocks and colluvial surficial materials located below the headscarp were mobilized in the debris flow, travelling a horizontal distance of 2050 m and descending 515 m in elevation into Little Salmon Lake, *i.e.,* a ΔH/L ratio of 0.25. A conservative estimate of the volume of material involved is on the order of 1 Mm^3, assuming a 2 m deposit thickness across a 400 000 m^2 area. Numerous large trees with trunks up to 50 cm in diameter were pushed over and deposited along the margins of the lower debris flow.

Figure 2. *View of the Little Salmon Lake landslide.*

The bedrock material associated with the original slope failure is part of the Snowcap Assemblage, which regionally consists of psammitic schist, quartzite, dark grey carbonaceous schist, calc-silicate rocks, minor amounts of marble, and local amounts of amphibolite, greenstone and ultramafic rocks of Devonian age and older (Colpron *et al.*, 2002; Piercey and Colpron, 2009).

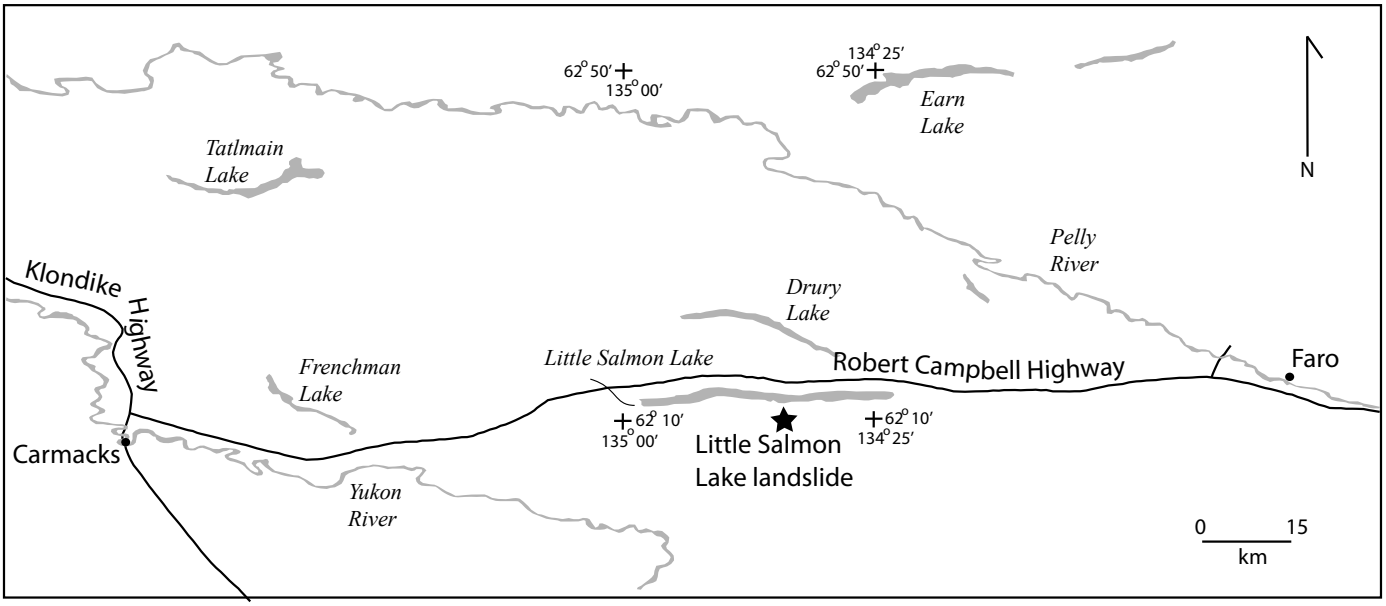

Figure 1. *Location of the Little Salmon Lake landslide.*

DESCRIPTION OF THE DEPOSIT AND ITS PROPERTIES

The upper part of the landslide deposit consists of tens of large slump blocks, most of which are still vegetated (Fig. 3). The slumped blocks have dimensions on the order of 10 x 10 x 20 m (height x length x width). Two sag ponds were observed behind slumped blocks on the western upper portion of the deposit. Hundreds of conical mounds of distinctly variable colour and varying in height from 0.3 m to 10 m (Fig. 4) comprise the central and lower sections of the deposit. A great majority of the mounds are composed of disintegrated bedrock of unimodal lithology, including yellow quartzite, grey schist and dark grey graphitic schist while others are composed of brown gravel-size surficial material. Where the material in the mounds is derived from two lithologies, the contact between them is sharp (Fig. 5). Some mounds have a thin layer of tephra at their pinnacle. The materials comprising the mounds are generally clast-supported, although occasionally consist of exclusively fine-grained clay-rich material. The clasts primarily consist of medium gravel to small cobbles, with occasional larger cobbles up to 50 cm. The average slope angle of the conical features is between 35° and 37° (Fig. 6a). These values correlate with the angle of repose of gravel which is reported to be between 35° and 40°. Field assessment of the density categories for the conical landforms revealed that they could be excavated with a shovel (S2 and S3) while some needed a pick for excavation (S4) (classification from BC Ministry of Forests, 2002; Fig. 6b).

Figure 3. *Slumped block of broken bedrock in the upper section of the landslide deposit.*

PERMAFROST AND GROUND ICE

A reconnaissance visit was made at the landslide on September 18, 2008. At that time, frost probing in the undisturbed mature spruce forest adjacent to the lower landslide deposit revealed an active layer that varied in thickness from 51 to 65 cm. Large angular blocks of ice-rich stratified colluvium up to 11 m in height were also noted in the landslide deposit (Fig. 7). Clastic material was actively ravelling from these blocks as they rapidly thawed, which prevented detailed investigations at the time. It was noted that the ravelling fragments were accumulating at the base of the frozen blocks in a conical form. Segregated ice content was visually estimated to be 50% in an approximately 9 m tall block. Frozen blocks were not observed when the site was next visited in July 2009.

Figure 4. *Conical mounds in the central and lower portion of the landslide deposit. Helicopter circled for scale.*

Figure 5. *Conical mound with bi-modal lithologies (graphitic schist and quartzite).*

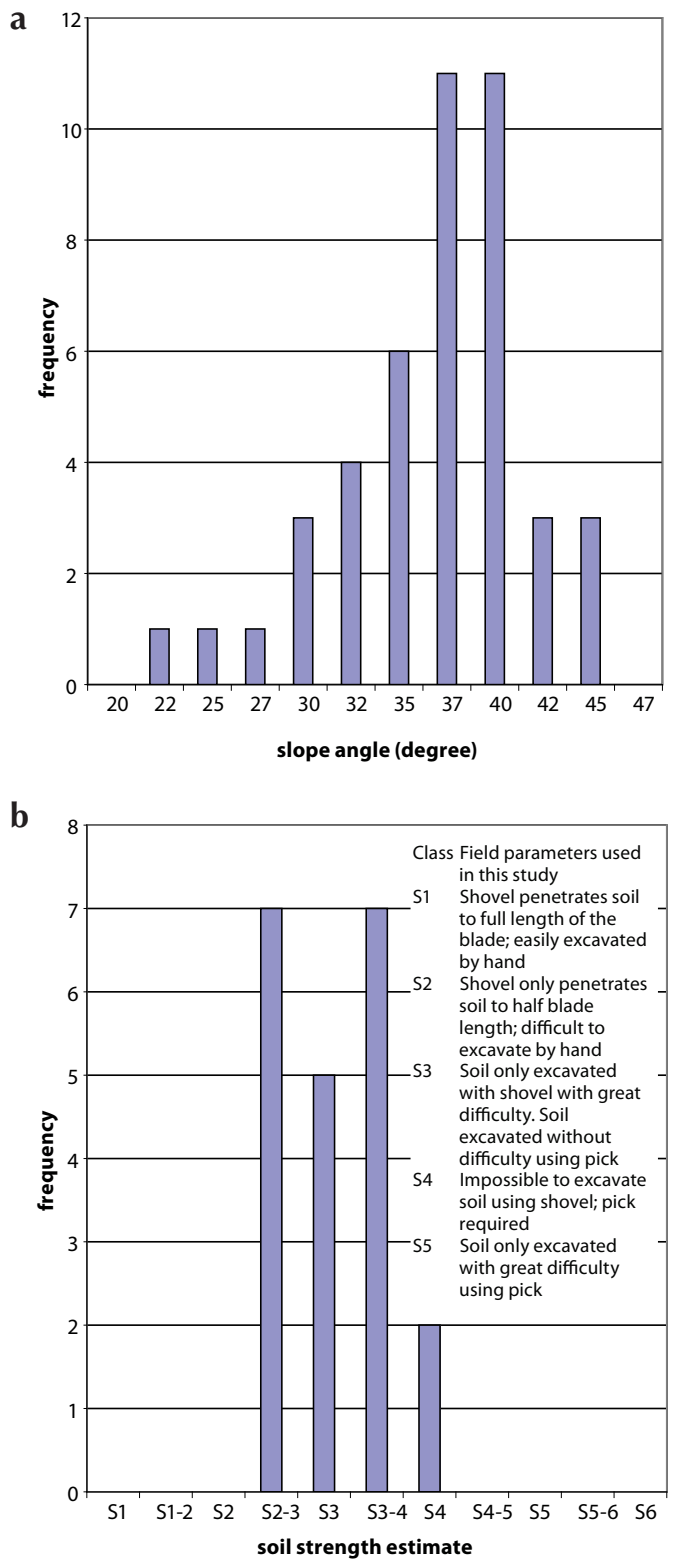

Figure 6. *(**a**) Histogram of the slope angle of the sides of the conical mounds, (**b**) Material strength categories of the conical mounds.*

Ten conical mounds (of varying sizes) were excavated to 0.5 m depth during the week of July 5, 2009 and no ice was observed in them at that time. Soil temperatures were measured (using a household-grade thermometer) at a depth of 0.5 m in these mounds and were found to be 8°C while the ambient air temperature was 23°C. A solid ice lens approximately 10 cm thick was, however, identified in a fractured bedrock slump block found in the upper part of the deposit (Fig. 8).

Figure 7. *Frozen angular block of surficial material observed in 2008 in the landslide debris. Person circled for scale.*

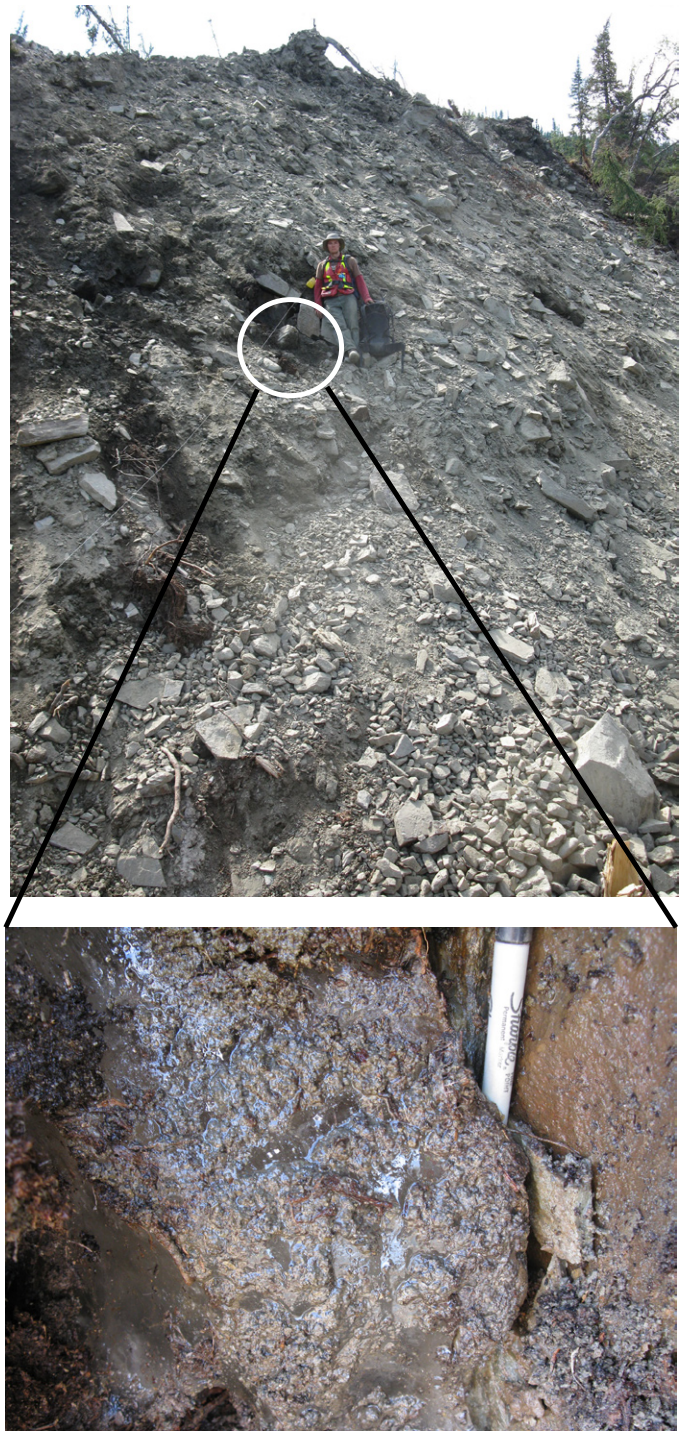

Figure 8. *Ice lens observed at the front of a slumped block of highly broken-up schist.*

FORMATION OF CONICAL MOUNDS

The presence of conical mounds in large landslide deposits has long been noted in landslide research, and the features are commonly referred to as molards (McConnell and Brock, 1904; Griggs, 1920; Shreeve, 1966). Several mechanisms for the formation of these landforms have been proposed, as summarized below.

1. Finer debris accumulates around a large boulder core as the landslide comes to rest (Goguel and Pachoud, 1972).
2. The mounds are formed by the vibration of the ground beneath a large landslide (Cassie *et al.*, 1988).
3. Formation of the mounds may be associated with the presence of a cohesive layer between two frictional layers in the original failed material (Shea and van Wyk de Vries, 2008). This heterogeneity leads to a differential deformation rate which in turn results in the formation of hummocks.
4. The mounds form when the velocity of the debris in the flow direction is less than the velocity perpendicular to the flow direction (Dufresne and Davies, 2009).
5. In landslides involving saturated fine-grained material, the mounds are formed from sand or silt boils associated with the release of excess pore pressure (Evans *et al.*, 2009).

The presence of tephra caps on some of the mounds, the dominantly unimodal lithological composition, or sharp contact between lithologies in the case of bimodal mounds and the internal structures (sharp contact between lithologies and stratification in mounds composed of surficial material), all argue against a turbulent or pore pressure release of liquefied material as an emplacement mechanism. The accumulation of surficial material around a boulder core as a formation mechanism is also inconsistent with our field observations. The mechanism we suggest for the formation of the conical mounds at the Little Salmon Lake landslide is that cohesive or frozen blocks of surficial material and fractured rock are mobilized by high pore water pressure in the surrounding saturated sediments. These blocks are rafted downslope in the main body of the landslide and subsequently melted and/or dried to form conical features after they have come to rest in the deposit zone. In this proposed mechanism, the ice would provide the cohesion in a fashion similar to the wet sand in the physical models of Shea and van Wyk de Vries (2008).

ROCK MASS

The rock mass quality was assessed using the Geological Strength Index (GSI) which was originally proposed by Hoek and Brown (1997) and later modified by Marinos and Hoek (2000). The GSI chart provides a quantification of the rock mass quality based on field observations of the structure present in the rock mass and the surface condition of the discontinuities. The applications and limitations of the GSI approach are discussed in Marinos *et al.* (2005) and Brown (2008). The rock mass quality as observed in the headscarp and sidescarps was low, corresponding to a range between 30 and 45 on the GSI chart (Fig. 9). The rock mass has a persistent and pervasive schistose foliation and four discontinuity sets

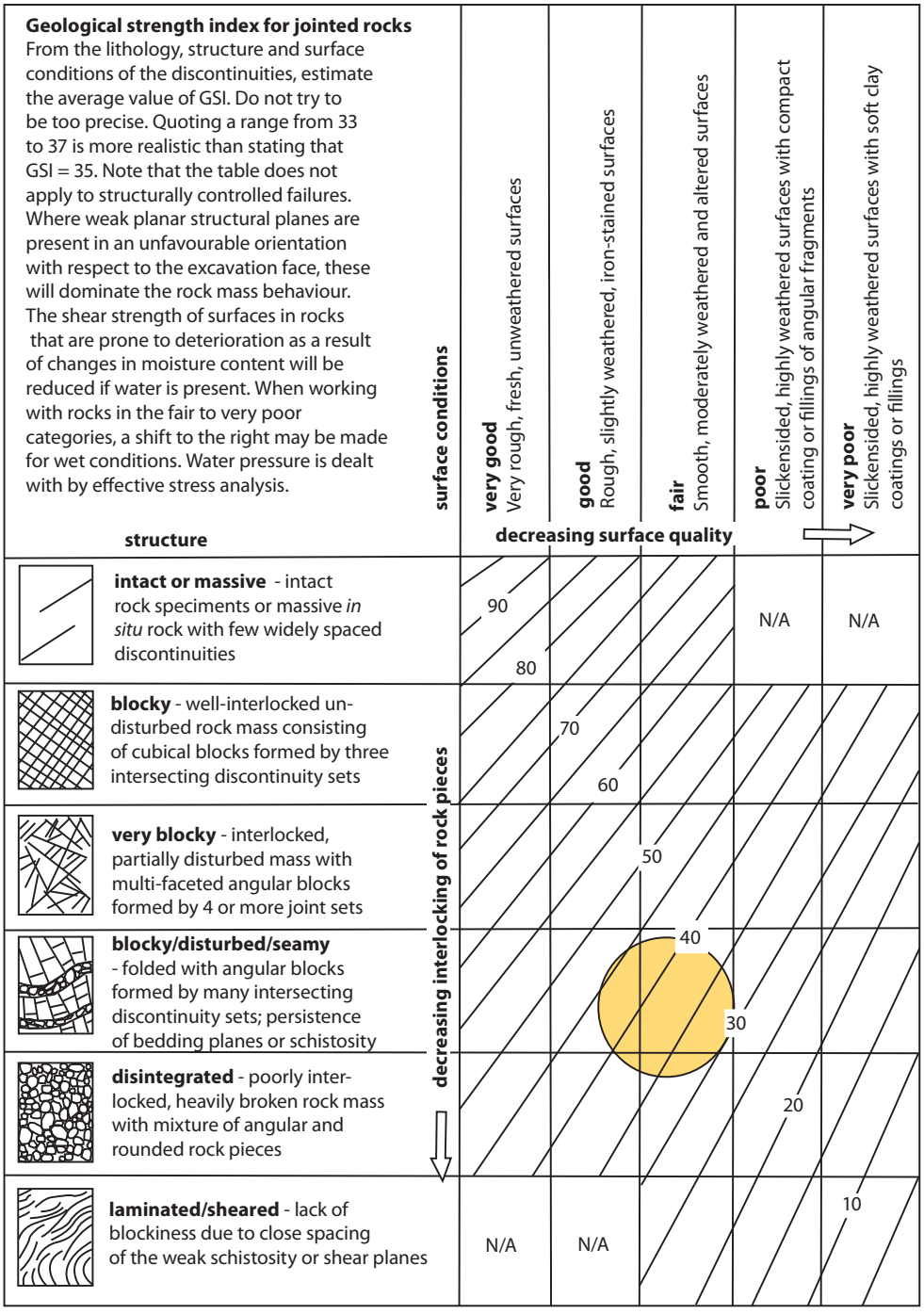

Figure 9. *Geological Strength Index chart highlighting the range of rock mass quality observed in the headscarp and sidescarp of the Little Salmon Lake landslide.*

which places it at the intersection of the very blocky and blocky/disturbed/seamy rock mass structure categories. Zones of intense weathering often correspond to graphite-rich layers. The discontinuity surface conditions were dominantly fair in the schistose units with some good conditions in the quartzite layers. Such low rock mass qualities are typically associated with zones of tectonic deformation and/or zone of intense alteration and weathering. This could not be rigorously confirmed at the Little Salmon Lake landslide due to the active rockfall activity which restricted access to the headscarp. Groundwater seepage was also observed in various parts of the headscarp and sidescarps. The low rock mass quality suggests that the slope stability is, at least in part, controlled by the rock mass strength.

KINEMATIC ANALYSIS

A limited number (N = 87) of discontinuity (foliation and joints) orientation measurements were acquired in the sidescarp of the landslide and used to conduct a kinematic analysis. A kinematic analysis is a geometric test, which uses for the average slope orientation an assumed discontinuity friction angle and the discontinuity measurements to assess the feasibility of simple failure mechanisms (Fig. 10). The stereographic techniques used to kinematically assess the feasibility of the planar, wedge and toppling failure mechanisms are outlined in Wyllie and Mah, 2004. Poles (Figs. 10a and 10c) or intersection of planes (Fig. 10b) which fall within the shaded area of the stereonets indicate a feasible failure mechanism. The results suggest that planar sliding (Fig. 10a) and wedge failures (Fig. 10b) are feasible with an assumed 40° slope angle and a 30° friction angle (angle at which a block would slide along an inclined plane) along the discontinuity surfaces. Only one discontinuity falls within the toppling envelope (Fig. 10c).

SUMMARY

The 2008 reactivation of the Little Salmon Lake landslide primarily involved the mobilization of debris from a previous slope failure at the same location. The surface of

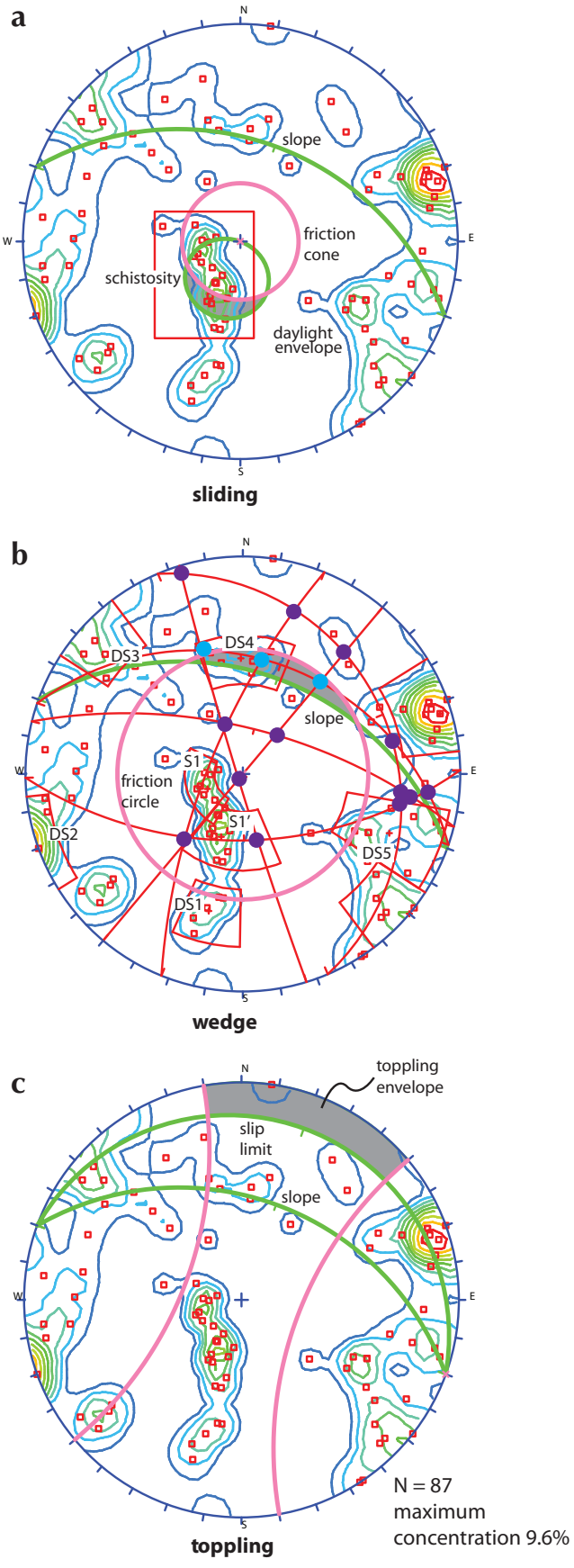

Figure 10. *Summary of the kinematic analysis performed on the poles to the discontinuities measured in the sidescarp of the Little Salmon Lake landslide.* ***(a)*** *sliding,* ***(b)*** *wedge,* ***(c)*** *toppling failure mechanism (lower hemisphere projection, equal angle stereonet).*

the latest landslide deposit is distinctly characterized by hundreds of conical mounds up to 10 m tall. The most likely mechanism of mound formation is that blocks of frozen colluvium or heavily fractured bedrock moved downslope as coherent masses and subsequently melted into cones with slopes at their angle of repose. The slope stability conditions of the initial Little Salmon Lake landslide were probably controlled by both the rock mass strength (as suggested by the low rock mass quality observed) and by the discontinuities present (suggesting planar sliding and wedge failures).

It is important to note that the geomorphic setting of the Little Salmon Lake landslide is not unique to the area and at least two other large permafrost-related landslides are found within 20 km of this landslide (Lyle, 2006). The fact that pre-existing landslide debris can be reactivated in large destructive landslides has serious implications concerning the location of future development in similar geomorphic settings. The south shore of Little Salmon Lake was intensely burned in a severe forest fire during the summer of 2009 which may significantly affect future slope stability in the area due to altered ground temperature, loss of soil strength associated with the vegetation and soil moisture conditions. A reconnaissance flight on September 25, 2009 revealed that the entire forest surrounding the Little Salmon Lake fire had been completely burned and that numerous shallow landslides had recently occurred on nearby slopes.

MOUNT STEELE 2007 ROCK AND ICE AVALANCHE

INTRODUCTION

On July 24 2007, a large rock and ice avalanche occurred on Mount Steele, located in an uninhabited area of the Kluane National Park in southwestern Yukon (Fig. 11). The mountain lies within the Icefield Ranges of the St. Elias Mountains. The slope failure was on the north face of the mountain (Fig. 12) which has been regionally mapped within a belt of Late Miocene Wrangell Suite granodiorite, diorite and gabbro lithologies (Dodds and Campbell, 1992). Hornblende-biotite-quartz diorite, tonalite and plagioclase-hornblende-biotite porphyry lithologies were observed in rock fragments collected in the deposit zone (Lipovsky *et al.*, 2008a).

Several smaller avalanches were noted in the weeks leading up to the July 24th event. The main and preceding events have been described by Lipovsky *et al.* (2008a,b).

The debris travelled 5.76 km horizontally with a vertical descent of 2160 m for a resultant ΔH/L ratio of 0.32. The seismic record suggests that the main event lasted approximately 100 seconds and consequently the minimum average velocity of the avalanche was 35 m/s.

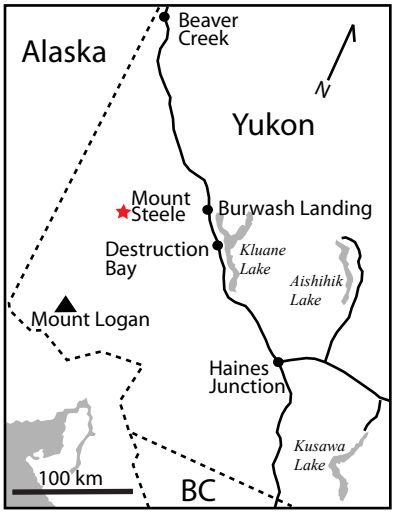

Figure 11. *Location of the Mount Steele rock and ice avalanche.*

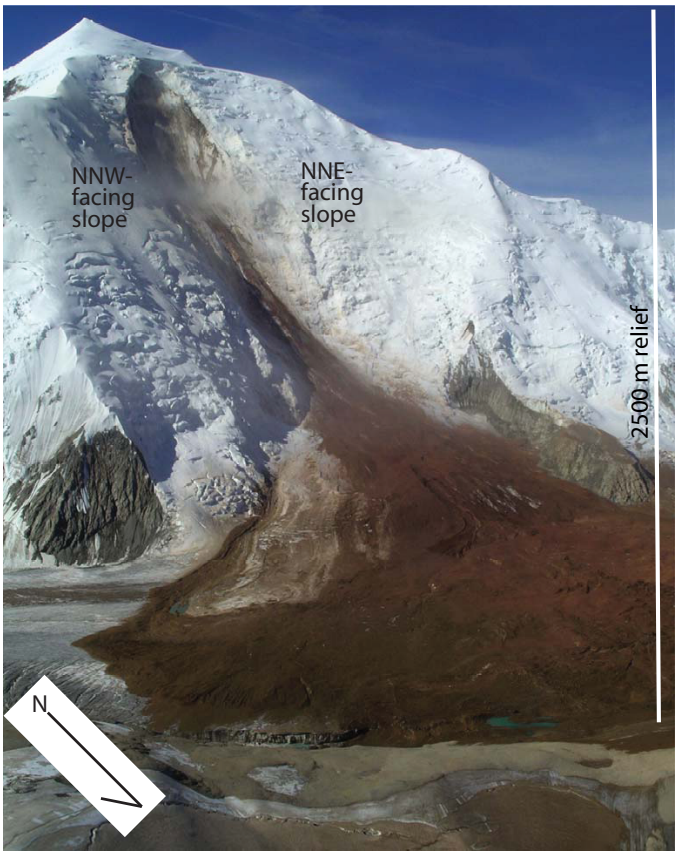

Figure 12. *View of the Mount Steele rock and ice avalanche.*

The debris covered an area of 3.66 km^2 with a thickness varying between 4 and 22 m, which suggests a bulked volume between 27.5 and 80.5 Mm^3. The failures are not thought to have been triggered by earthquakes or the warmer-than-average, but not abnormally warm temperatures that occurred in the 10 days prior to the main failure.

DISCONTINUITY ANALYSIS USING COLTOP-3D

The software COLTOP-3D (Jaboyedoff *et al.,* 2004) was used to derive surface orientation based on airborne-LiDAR DEM of the Mount Steele area. COLTOP-3D assigns a colour to each cell in the DEM based on the dip and dip direction orientation of its pole. Zones of constant orientation are highlighted and assumed to represent a structural surface in the bedrock such as bedding, persistent joints and/or faults. These zones of constant orientation are manually identified by the user. COLTOP-3D has been previously used on several rock slope stability case studies (Derron *et al.*, 2005; Pedrazzini *et al.*, 2008; Jaboyedoff *et al.*, 2009; Metzger *et al.*, 2009). Due to the extensive ice cover in the study area, surface orientations could only be obtained from the initiation zone of the landslide and from the east-facing rock wall in the gully that the landslides followed (Fig. 13).

Three discontinuity sets (DS1, DS2, DS3) were identified in the landslide scarp using COLTOP-3D (Fig. 14). They correspond to the discontinuities identified by Lipovsky *et al.* (2008a). DS3 may have a subset with a steeper dip, which is shown as DS3' in Figure 14. Two other discontinuity sets (DS4 and DS5) were also noted in

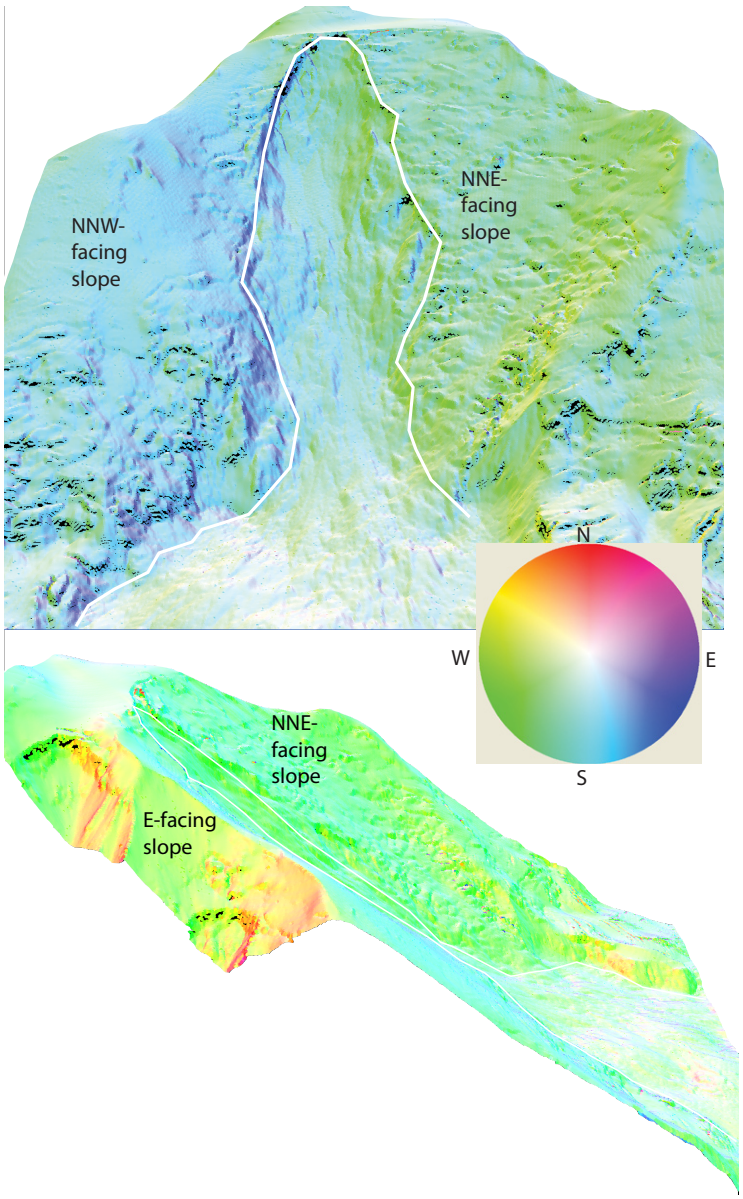

Figure 13. *COLTOP-3D rendered view where the digital elevation model is coloured as a function of the dip and dip direction of each cell. The inset stereonet provides the colour coding for the surfaces.*

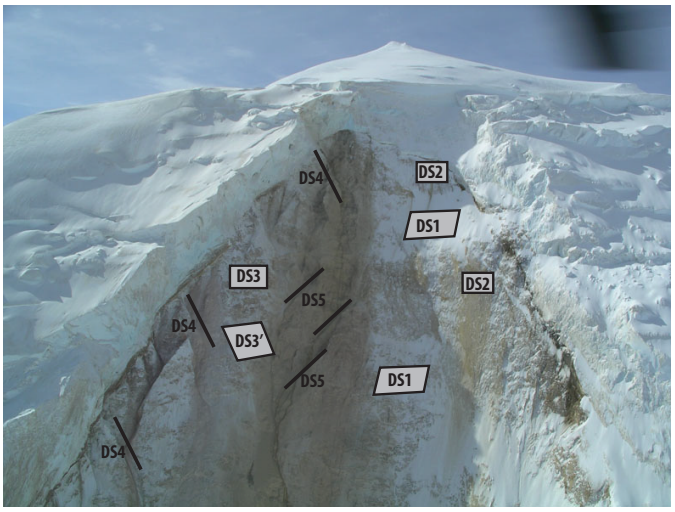

Figure 14. *Headscarp of the Mount Steele rock and ice avalanche with the identified discontinuities annotated.*

photographs of the headscarp but are dipping into the slope and therefore cannot be resolved in the landslide scar using COLTOP-3D. Upon further investigation of the east-facing gully wall using the LiDAR-derived DEM of Mount Steele, two more surfaces were recognized having orientations consistent with the planes (DS4 and DS5) highlighted in the photograph (Fig. 14).

KINEMATIC ANALYSIS

A preliminary kinematic analysis was performed using a friction angle of 30° along the discontinuity surfaces. Since the failure occurred in a broad gully, two slope surfaces were considered in this analysis. The pre-failure topography was approximated by projecting the orientation of the slope on either side of the landslide source zone into the existing landslide scar. Two such surfaces were defined using COLTOP-3D: a north-northeast wall with dip/direction 42°/018° and a north-northwest wall with dip/direction 45°/340°. The kinematic analysis revealed that sliding failure was feasible on DS1 in the north-northeast wall (Fig. 15a) as suggested by Lipovsky *et al.* (2008a) and that sliding was only marginally feasible on DS1 and DS3 in the north-northwest wall. Wedge failures were feasible along

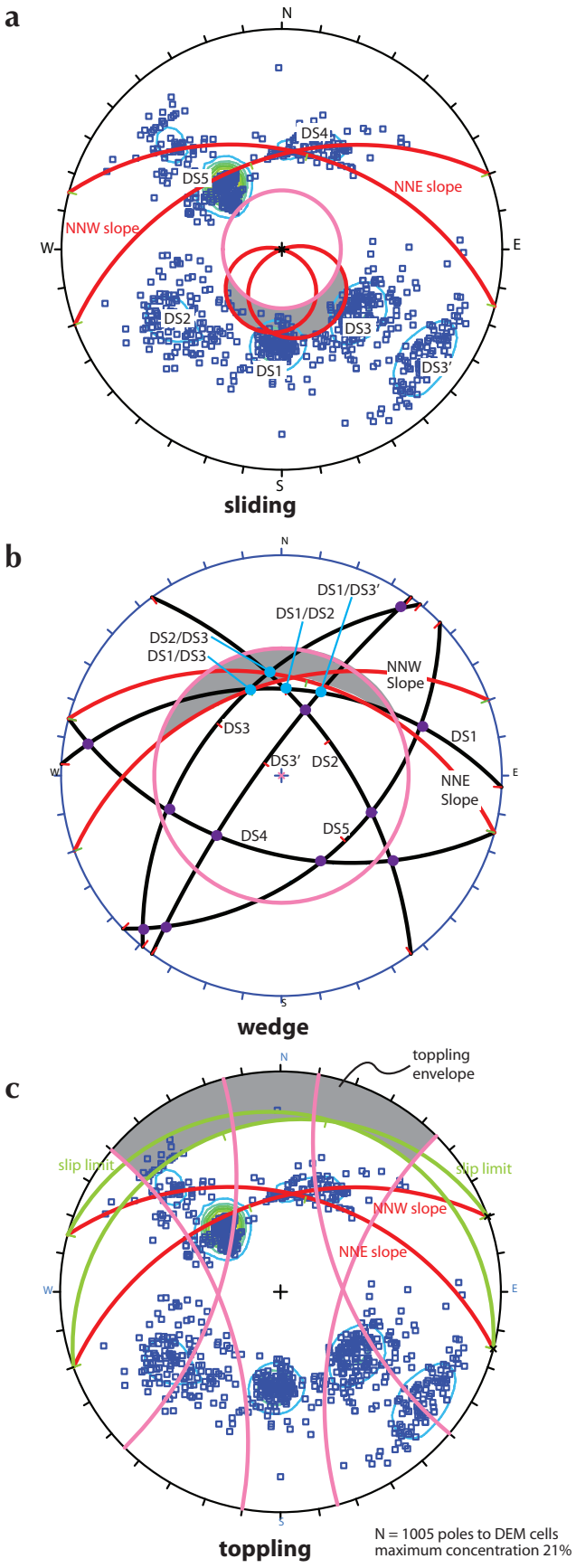

Figure 15. *Summary of the Mount Steele kinematic analysis performed on the poles to the surfaces obtained using COLTOP-3D.* ***(a)*** *sliding,* ***(b)*** *wedge,* ***(c)*** *toppling failure mechanism (lower hemisphere projection, equal angle stereonet).*

Table 1. *Summary of the surface wedge combination analysis conducted using the software Swedge.*

	Slope face orientation (dip/dip direction)	
	42°/014° north-northeast	45°/340° north-northwest
Number of combinations	504510	504510
Number of valid wedges	123726	98085
Number of stable wedges	114825 (93%)	77573 (79%)
Number of failed wedges	8901 (7%)	20512 (21%)
Cumulative weight of wedges with FOS<2 (tones)	317E6	429E6

intersections between DS1 and DS3 and DS2 and DS3 in the north-northwest wall; they were only marginally feasible along the intersections between DS1 and DS3′ and between DS2 and DS3 in the north-northeast wall and between DS1 and DS2 in the north-northwest wall (Fig. 15b). Toppling was shown to be marginally feasible along discontinuity orientations which represent outliers to DS5 in the north-northwest wall (Fig. 15c).

SURFACE WEDGE ANALYSIS

The limit equilibrium code "Swedge" (Rocscience, 2006) was used to investigate the stability of rock wedges in the various rock slope walls on the northern face of Mount Steele. The combination analysis in Swedge applies a user defined list of discontinuities to calculate the factor of safety (FOS) for each valid wedge intersection for a given slope face. The results of the combination analysis are based on the surface orientations obtained using COLTOP-3D. The analysis was carried out assuming a 30° friction angle on all discontinuity surfaces and a maximum discontinuity persistence of 100 m. The summary of the Swedge combination analyses (Table 1) suggests more wedges and a potentially larger cumulative volume of wedges with a FOS <2 on the north-northwest wall than on the north-northeast wall. The FOS <2 was chosen as a conservative threshold for the calculated stability conditions of the wedges to account for the uncertainty associated with friction angle along the discontinuity surface, discontinuity persistence, the natural variability in the slope face orientation and the pore water pressure conditions in the ice/rock mass.

THREE-DIMENSIONAL DISTINCT ELEMENT ANALYSIS

3DEC (Itasca, 2008) is a three-dimensional distinct element code which represents a rock mass as a collection of blocks bounded by planes (*i.e.*, discontinuities). The constitutive model (rigid, elastic, elasto-plastic), the strength of the material inside the blocks and the shear and tensile strength along the surfaces bounding the blocks can be specified by the user. 3DEC allows for large displacement and rotation of the modelled blocks. More information about 3DEC can be obtained in Cundall (1988) and Hart *et al.* (1988). Preliminary 3DEC models were constructed using rigid blocks and an assumed 30° friction angle along all discontinuities. The geometry of the north face of Mount Steele was modelled as two planes (north-northeast and north-northwest walls) approximating the pre-failure topography of the broad gully as previously described. The spacing of all discontinuity sets in these preliminary models was assumed to be 75 m. The first model assumed that only DS1, DS2, DS3 and DS3′ were present, which resulted in a large failure on the north-northwest-facing slope (Fig. 16a). The second model incorporated all six identified discontinuity sets (DS1, DS2, DS3, DS3′, DS4 and DS5). As in the previous model a large failure was modelled on the north-northwest-facing slope (Fig. 16b). The results demonstrate that DS1, DS2, DS3 and DS3′ play an important role in the stability of the models while DS4 and DS5 appear to be less important. The rock slope failures in both models appear to be restricted to the north-northwest-facing slope.

DISCUSSION

The kinematic, Swedge and 3DEC analyses all suggest that the north-northwest-facing wall (or east side) is the least stable of the two main faces present on the north side of Mount Steele. That is in contrast with the observed failure which occurred at the intersection of the north-northeast and north-northwest-facing walls. This could be due to the fact that the model does not incorporate other factors which may have played an important role in the failure, such as ice cover, groundwater influence and the presence of a large tectonic structure or zone of low rock-mass quality which could not be identified using COLTOP-3D due to the thick ice cover. For example, the Mount Steele landslide may have initiated as an ice avalanche which "plucked" and entrained the underlying rock mass. A large rock and ice avalanche similar to the Mount Steele landslide occurred in 2005 at Mt. Steller in

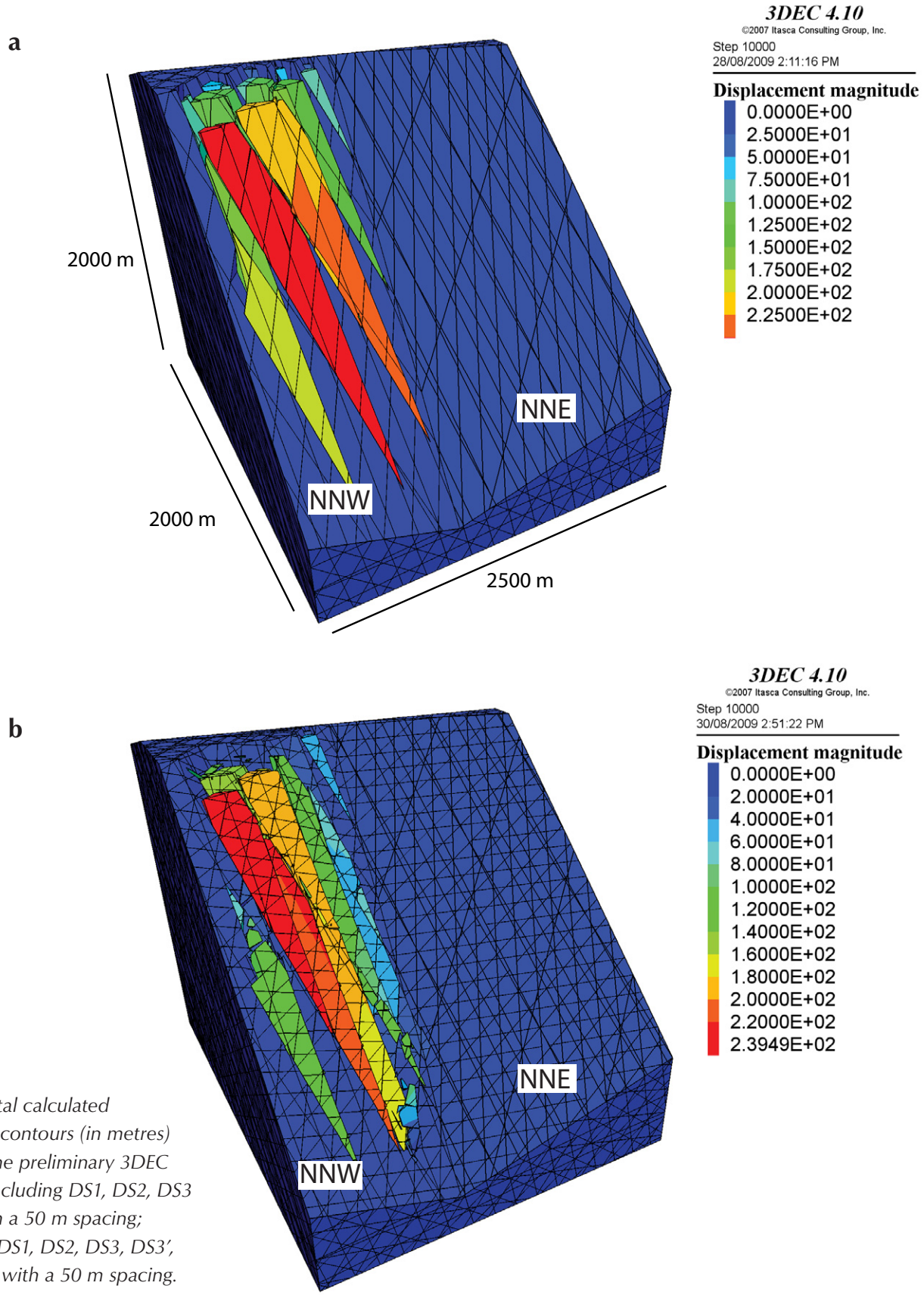

Figure 16. *Total calculated displacement contours (in metres) obtained in the preliminary 3DEC models;* ***(a)*** *including DS1, DS2, DS3 and DS3′ with a 50 m spacing;* ***(b)*** *including DS1, DS2, DS3, DS3′, DS4 and DS5 with a 50 m spacing.*

Alaska (Huggel *et al.*, 2008). Investigators conducted thermal modelling which highlighted that a hanging glacier in the summit area may have promoted warmer ground temperatures and reduced the stability of the underlying permafrost (Huggel *et al.*, 2008). A similar hanging glacier appears to have been present on the north face of Mount Steele and thermal modelling should be included in further slope stability investigations of the site. Finally, it should be highlighted that the quality of the remotely acquired discontinuity orientation data was not verified using other techniques (*e.g.,* ground measurements, photogrammetry or ground-based LiDAR). This introduces a certain degree of uncertainty in the subsequent slope stability analyses, but in remote and inaccessible study sites such as Mount Steele it is not always possible or feasible to obtain alternate data.

SUMMARY

The orientation of very high persistence discontinuity surfaces (>20 m long; ISRM, 1978) in the 2007 Mt. Steele landslide initiation zone were successfully measured from airborne-LiDAR-generated DEM using the software COLTOP-3D. These surface orientations were consistent with discontinuity sets previously identified in photographs of the failure headscarp. The surface orientations were subsequently used to perform a preliminary investigation of slope stability controls at the study area. All analyses suggest that the north-northwest-facing portion of Mount Steele's north face is the least stable. This is inconsistent with the observed failure which occurred at the intersection between north-northeast and north-northwest-facing slopes. This discrepancy highlights that other factors, such as ice cover morphology, groundwater conditions and rock mass strength which were not included in the preliminary slope stability models, may have been more important contributing factors to the 2007 rock and ice avalanches on Mount Steele.

CONCLUSION

This paper presents a preliminary description and slope stability analyses of two recent large landslides in Yukon. The first section of this paper describes some distinctive surface features present in the 2008 Little Salmon Lake landslide deposit. Hundreds of conical mounds in the deposit were found to be dominantly composed of material derived from a unimodal lithology. They varied in height from 0.3 to 10 m and had an average slope angle between 35° and 37°. Field observations suggest that the mounds were not formed from rapid and turbulent transport or deposition. Rather they suggest that frozen blocks of surficial material and fractured rock were mobilized by surrounding saturated sediments with high pore water pressure. Once the blocks came to rest in the deposit zone, they subsequently melted forming conical mounds shape. The rock mass in the headscarp of the Little Salmon Lake landslide was described using the Geological Strength Index (GSI) and was found to be of low quality.

The second section presents a preliminary slope stability analysis of the June 2007 Mount Steele rock and ice avalanche. An airborne-LiDAR digital elevation model (DEM) was used in conjunction with the software COLTOP-3D to obtain the orientation of very high persistence (>20 m) surfaces. These surfaces were assumed to represent discontinuities in the rock mass and their orientation was subsequently used to conduct slope stability analyses. All the analyses performed suggest that a slope failure was more likely to occur on a different portion of Mount Steele's north face than what actually occurred in 2007. This suggests that external factors not incorporated into the analyses (such as high pore water pressure, the influence of the overlying glacier and/or low rock mass strength resulting from tectonic damage, alteration and weathering), played a greater role in causing the 2007 rock and ice avalanches than the structural characteristics of the local bedrock. All of these scenarios should be considered in future investigations.

ACKNOWLEDGEMENTS

The authors would like to thank Tim Sivak (2009) and Kristen Kennedy (2008) for their assistance in the field at the Little Salmon Lake landslide and Ryan Lyle, Jean Hutchinson and Brent Ward for discussions on slope stability in the Little Salmon Lake area. Funding for this project was provided by the Yukon Geological Survey, Northern Scientific Training Program, NSERC and an SFU graduate fellowship. Matthieu Sturzenegger provided a critical review of the manuscript.

REFERENCES

BC Ministry of Forests, 2002. Forest Practices Code of British Columbia - Forest Road Engineering Guidebook Second Edition. Government of British Columbia, Victoria, BC, 218 p.

Brown, E.T., 2008. Estimating the mechanical properties of rock masses. *In:* Southern Hemisphere International Rock Mechanics Symposium 2008, Y. Potvin, J. Carter, A.V. Dyskin and R. Jeffrey (eds.), Perth, Australia, p. 3-22.

Cassie, J.W., van Gassen, W. and Cruden, D.M., 1988. Laboratory analogue of the formation of molards, cones of rock-avalanche debris. Geology, vol. 16, p. 735-738.

Colpron, M., Murphy, D.C., Nelson, J.L., Roots, C.F., Gladwin, K., Gordey, S.P., Abbott, G. and Lipovsky, P.S., 2002. Preliminary geological map of Glenlyon (105L/1-7, 11-14) and northeast Carmacks (115I/9, 16) areas, Yukon Territory (1:125 000 scale). Indian and Northern Affairs Canada, Exploration and Geological Services Division, Yukon Region, Open File 2002-9, 1:150 000 scale.

Cundall, P.A., 1988. Formulation of a three-dimensional distinct element model - Part I. A scheme to detect and represent contacts in a system composed of many polyhedral blocks. International Journal of Rock Mechanics and Mining Sciences & Geomechanics Abstracts, vol. 25, no. 3, p. 107-116.

Derron, M.-H., Jaboyedoff, M. and Blikra, L.H., 2005. Preliminary assessment of rockslide and rockfall hazards using a DEM (Oppstadhornet, Norway). Natural Hazards and Earth System Science, vol. 5, no. 2, p. 285-292.

Dodds, C.J. and Campbell, R.B., 1992. Geology of Mount St. Elias map area (115B and C[E1/2]), Yukon Territory. Geological Survey of Canada, Open File 2189, 85 p.

Dufresne, A. and Davies, T.R., 2009. Longitudinal ridges in mass movement deposits. Geomorphology, vol. 105, no. 3-4, p. 171-181.

Evans, S.G., Roberts, N.J., Ischuk, A., Delaney, K.B., Morozova, G.S. and Tutubalina, O., 2009. Landslides triggered by the 1949 Khait earthquake, Tajikistan and associated loss of life. Engineering Geology, vol. 109, no. 3-4, p. 195-212.

Goguel, J. and Pachoud, A., 1972. Géologie et dynamique de l'écroulement du Mount Granier, dans le Massif de Chartreuse, en novembre 1248, Bulletin du Bureau de Recherche Géologique et Minière vol. 1, p. 29-38.

Griggs, R.F., 1920. The great Mageik landslide. The Ohio Journal of Science, vol. 20, no. 8, p. 325-354.

Hart, R.D., Cundall, P.A. and Lemos, J.V., 1988. Formulation of a three-dimensional distinct element model - part II: Mechanical calculations for motion and interaction of a system composed of many polyhedral blocks. International Journal of Rock Mechanics and Mining Sciences & Geomechanics Abstracts, vol. 25, no. 3, p. 117-125.

Hoek, E. and Brown, E.T., 1997. Practical estimates of rock mass strength. International Journal of Rock Mechanics and Mining Sciences, vol. 34, no. 8, p. 1165-1186.

Huggel, C., Caplan-Auerbach, J., Gruber, S., Molnia, B.F. and Wessels, R.L., 2008. The 2005 Mt. Steller, Alaska, rock-ice avalanche: A large slope failure in cold permafrost. *In:* 9th International Conference on Permafrost, D.L. Kane and K. Hinkel (eds.), Fairbanks, Alaska, p. 747-752.

ISRM, 1978. Suggested methods for the quantitative description of discontinuities in rock masses. International Journal of Rock Mechanics, Mining Sciences and Geomechanics Abstract, vol. 15, p. 319-368.

Itasca, 2008. 3DEC v. 4.1, Itasca Consulting Group, Minneapolis, Minnesota

Jaboyedoff, M., Baillifard, F., Couture, R., Locat, J., Locat, P. and Rouiller, J.-D., 2004. New insight of geomorphology and landslide prone area detection using DEM. *In:* 9th International Symposium on Landslides, W.A. Lacerda, M. Ehrlich, A.B. Fontoura and A. Sayo (eds.), Balkema, p. 199-205.

Jaboyedoff, M., Couture, R. and Locat, J., 2009. Structural analysis of Turtle Mountain (Alberta) using digital elevation model: Toward a progressive failure. Geomorphology, vol. 103, no. 1, p. 5-16.

Lipovsky, P.S., Evans, S.G., Clague, J.J., Hopkinson, C., Couture, R., Bobrowsky, P., Ekström, G., Demuth, M.N., Delaney, K.B., Roberts, N.J., Clarke, G. and Schaeffer, A., 2008a. The July 2007 rock and ice avalanches at Mount Steele, St. Elias Mountains, Yukon, Canada. Landslides, vol. 5, no. 4 p. 445-455.

Lipovsky, P.S., Evans, S.G., Clague, J.J., Hopkinson, C., Couture, R., Bobrowsky, P., Ekström, G., Demuth, M.N., Delaney, K.B., Roberts, N.J., Clarke, G. and Schaeffer, A., 2008b. Reconnaissance observations of the July 24, 2007 rock and ice avalanche at Mount Steele, St. Elias Mountains, Yukon, Canada. *In:* 4th Canadian Conference on Geohazards: From Causes to Management, J. Locat, D. Perret, D. Turmel, D. Demers and S. Leroueil (eds.), Quebec City, p. 323-330.

Lyle, R.R., Hutchinson, D.J. and Preston, Y., 2005. Landslide processes in discontinuous permafrost, Little Salmon Lake (NTS 105L/1 and 2), South-central Yukon. *In:* Yukon and Exploration Geology 2004, D.S. Emond, L.L. Lewis and G.D. Bradshaw (eds.), p. 193-204.

Lyle, R.R., 2006. Landslide susceptibility mapping in discontinuous permafrost: Little Salmon Lake, Central Yukon. Unpublished MSc thesis, Department of Geological Sciences and Geological Engineering, Queen's University, Kingston, Ontario, 366 p.

Marinos, P. and Hoek, E., 2000. GSI: A geologically friendly tool for rock mass strength estimation, *In:* GEOENG 2000, Technomic Publishing Co. Inc., Melbourne, Australia, p. 1422-1440.

Marinos, V., Marinos, P. and Hoek, E., 2005. The Geological Strength Index: Applications and limitations. Bulletin of Engineering Geology and the Environment, vol. 64, no. 1, p. 55-65.

McConnell, R.G. and Brock, R.W., 1904. Report on the great landslide at Frank, Alberta, 1903. Dominion of Canada, Department of the Interior, Annual report, 1903, part VIII, p. 3-17.

Metzger, R., Jaboyedoff, M., Oppikofer, T., Viero, A. and Galgaro, A., 2009. COLTOP-3D: A new software for structural analysis with high resolution 3D point clouds and DEM. *In:* Frontiers + Innovation: Canadian Society of Petroleum Geologists, Canadian Society of Exploration Geophysicists and Canadian Well Logging Society Joint Convention, Calgary, Alberta, p. 278-281.

Pedrazzini, A., Jaboyedoff, M., Froese, C., Langenberg, W. and Moreno, F., 2008. Structures and failure mechanisms analysis of Turtle Mountain. *In:* 4th Canadian Conference on Geohazards, J. Locat, D. Perret, D. Turmel, D. Demers and S. Leroueil (eds.), Quebec City, QC, p. 349-356.

Piercey, S.J. and Colpron, M., 2009. Composition and provenance of the Snowcap assemblage, basement to the Yukon-Tanana terrane, northern Cordillera: Implication for Cordilleran crustal growth. Geosphere, vol. 5 no. 5, p. 439-464.

Rocscience, 2006. Swedge v5.0, Rocscience Inc. Toronto, Ontario.

Shea, T. and van Wyk de Vries, B., 2008. Structural analysis and analogue modeling of the kinemetics and dynamics of rockslide avalanches. Geosphere, vol. 4 no. 4, p. 657-686.

Shreeve, R.L., 1966. Sherman Landslide, Alaska. Science, vol. 154, p. 1639-1643.

Wyllie, D.C. and Mah, C.W., 2004. Rock Slope Engineering, 4th Edition. SponPress, New York, 431 p.